conformational characteristics of local regions of tRNA and ribosomes during the various step of protein biosynthesis. The principal limitation of the method is the ingenuity of the researcher to synthesize and utilize the appropriate spin-label. The greater the specificity of the labeling and the smaller the perturbance it can create on the system, the richer will be the information from such a study.

Unraveling Reactions with Rotating Electrodes

Stanley Bruckenstein*

Chemistry Department, State University of New York at Buffalo, Buffalo, New York 14214

Barry Miller

Bell Laboratories, Murray Hill, New Jersey 07974

Received May 4, 1976

This Account describes how the rotating disk and allied techniques can be used to unravel complicated heterogeneous and homogeneous reactions. The rotating disk geometry permits precise hydrodynamic control of the flux of material to and from a reacting surface, and thereby provides the chemist with a unique experimental variable.[1,2] The application of this concept of flux control via hydrodynamics has been concerned, to date, principally with processes associated with electron transfer.

The rotating ring–disk electrode (RRDE) as conceived by Levich, Frumkin, and co-workers[3-5] provides the chemist with a powerful methodology for studying complicated chemical as well as electrochemical reactions. Prior work relied on single electrode techniques to elucidate the details of electrochemical reactions. However, such approaches can only give inferential evidence about the nature of the electrochemical reaction sequence involved. Supplementing such data with ex post facto information, for example, chemical analysis of the electrolyte, is often necessary, but is inadequate if an unstable or reactive species occurs during electrolysis.

The capability of a RRDE's ring electrode to detect, virtually simultaneously, species generated at the disk electrode provides an elegant and convenient solution to this analytical problem. In addition, the rigorously defined mathematics of the RRDE geometry makes it possible to distinguish between faradaic (electron transfer) and nonfaradaic processes.

In order to place the more recent work in perspective, we review classical rotating disk electrode (RDE) and RRDE theory and practice. Then the recent developments of hydrodynamically programmed RDE and RRDE are presented because of their power to discriminate further among subtly different reaction possibilities. Many of our illustrations involve metal deposition reactions and corrosion phenomena, but it should be kept in mind that the applications of rotating electrodes are much more general. Our object is to present a critical overview of the present state of rotating electrode methodology and to clarify the complementary nature of the various techniques.

Classical Rotating Electrodes

Figure 1 illustrates the geometry of all the rotating electrodes under discussion. P–P′ represents the plane of an insulating disk rotating about an axis O–O′ and containing a disk electrode of radius r_1. The typical streamlines for all electrodes obtained under laminar flow conditions are shown by the dotted lines with the arrowheads.

Rotating Disk Electrode. If the solution contains an electroactive species A, reaction 1 occurs at the disk

$$A + n_D e = B \qquad (1)$$

electrode if a suitable potential, E_D, is applied. It follows from Levich[1,2] that the resultant current for a disk electrode of radius r_1 is given by eq 2, where F is

$$i_D = 0.6025 n_D F \pi r_1^2 D^{2/3} \nu^{-1/6} \omega^{1/2} (C^b - C^s) \qquad (2)$$

the Faraday constant, D is the diffusion coefficient of species A (or B), ν is the kinematic viscosity, ω is the radian velocity of rotation, and C^b and C^s are the bulk and surface concentrations, respectively, of A (or B).

Curve I of Figure 2 represents the disk current–disk potential ($i_D - E_D$) curve that would be obtained for the reversible process in eq 1 in a supporting electrolyte containing only A in solution. The maximum disk current, $(i_D)_L$, occurring when C^s becomes vanishingly small, is remarkably reproducible and a valuable source of diffusion coefficients. An improved form of the

Stanley Bruckenstein is Professor of Chemistry at State University of New York at Buffalo. He received his B.S. degree at Polytechnic Institute of Brooklyn and his Ph.D. at the University of Minnesota. His research interests are in interfacial electrochemistry and electroanalytical chemistry, currently in the areas of underpotential metal deposition and trace electroanalysis.

Barry Miller is a member of the technical staff in the Chemical Physics Research Department at Bell Laboratories. He received his A.B. degree at Princeton and Ph.D. at MIT, and was a chemistry instructor at Harvard before joining Bell Laboratories. His research interests are in interfacial electrochemistry, currently in the areas of electrodeposition and solar energy conversion.

(1) V. G. Levich, *Acta Physiocochim. URSS*, **17**, 257 (1942).
(2) V. G. Levich, "Physicochemical Hydrodynamics", Prentice-Hall, Englewood Cliffs, N.J., 1962, p 60.
(3) R. M. Zaidel in ref 2, p 107.
(4) A. N. Frumkin, L. N. Nekrasov, V. G. Levich, and Yu. B. Ivanov, *J. Electroanal. Chem.*, 1, 84 (1959).
(5) A. N. Frumkin and L. N. Nekrasov, *Dokl. Akad. Nauk SSSR*, **126**, 115 (1959).

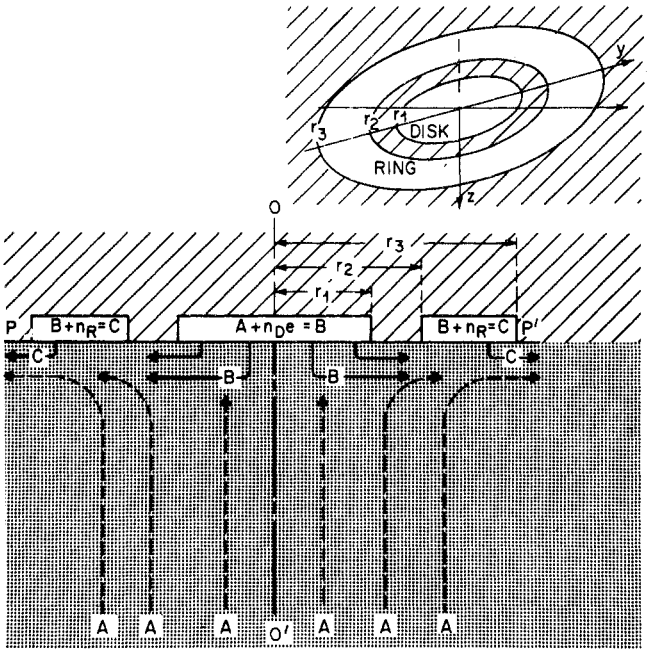

Figure 1. Rotating electrode geometry and flow patterns.

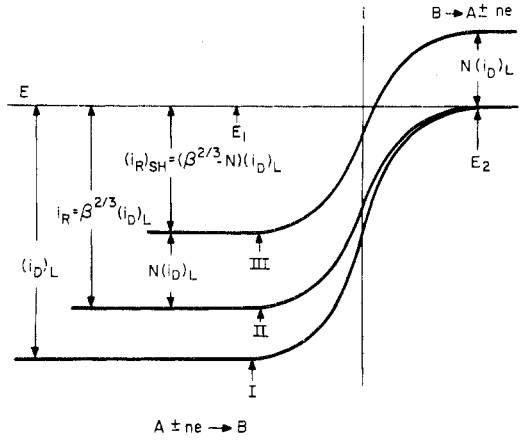

Figure 2. Ring and disk current–potential curves in solution of A. (I) Isolated disk; (II) isolated ring; (III) ring and disk. $\beta^{2/3} < 1$.

Levich equation derived by Newman should be used,[6,7] and simplified means of calculation[8] are available.

Rotating Ring Electrode. A rotating ring electrode of inner radius r_2 and outer radius r_3 is also shown in Figure 1. The ring electrode current in the absence of a disk, according to Levich and Zaidel,[3] is given by eq 3 for reaction 1 ($n_R = n_D$). The ring current–ring potential curve, curve II of Figure 2, has exactly the same shape as curve I obtained at a disk electrode. However, the ring current differs from the disk current by a factor, β, where

$$i_R = 0.6205 n_R F \pi (r_3^3 - r_2^3)^{2/3} D^{2/3} \nu^{-1/6} \omega^{1/2} \times (C^b - C^s) \quad (3)$$

$$\frac{i_R}{i_D} = \beta^{2/3} = \left[\frac{r_3^3}{r_1^3} - \frac{r_2^3}{r_1^3}\right]^{2/3} \quad (4)$$

(6) J. S. Newman, *J. Phys. Chem.*, 70, 1327 (1966).
(7) J. S. Newman, "Electrochemical Systems", Prentice-Hall, Englewood Cliffs, N.J., 1973, p 309.
(8) S. Bruckenstein, *J. Electrochem. Soc.*, 122, 1215 (1975).

Rotating Ring–Disk Electrode. A rotating ring–disk electrode is the composite structure shown in Figure 1. The occurrence of a ring electrode reaction does not affect currents at the disk electrode. However, the occurrence of a disk electrode reaction can cause a predictable change in the ring electrode current.

If reaction 1 occurs at the disk electrode, B is formed at the expense of A; then B escapes from the disk electrode by diffusion and is transported radially by the well-described convective transport occurring in the hydrodynamic boundary layer adjacent to the rotating disk. Thus, the solution normal to the ring electrode region contains the product of the disk reaction, B, in addition to A. However, this region is depleted in the concentration of A because of the conversion of some A into B at the disk electrode, as shown by the $(i_R)_{SH}$ level in curve III, Figure 2. Detecting B at the ring is known as a "collection" experiment; following the decrease in A at the ring is known as a "shielding experiment".

Collection–Intermediate Detection. For collection, the applied ring potential, E_R, is chosen so that reaction

$$B + n_R = C \quad (5)$$

5 occurs, where C may or may not be the same as A. (Note that we assume n_R and n_D are positive for reductions and negative for oxidations.) In this example, B leaves the disk electrode and is "collected" at the ring electrode as is depicted in Figure 1. If the disk current producing B is i_D and the ring electrode current "collecting" B is i_R, the "collection efficiency" N is

$$N = \frac{n_D}{n_R}\frac{i_R}{i_D} \quad (6)$$

N is a geometric property of a RRDE. Levich and Ivanov[4,5] originally obtained an approximate solution to the problem of calculating N, and later Albery and Bruckenstein[9] gave the rigorous solution. The first experimental verification of the RRDE system was by Frumkin and Nekrasov.[5]

Since the flux of B from the disk electrode under steady-state conditions is constant, it is a simple matter to obtain an i_R–E_R curve at the ring electrode by scanning the ring potential at a convenient rate. These data are frequently sufficient to identify the species B. Once this has been done, a suitable, constant ring potential can be chosen which will detect the species B, and then the potential of the disk electrode can be scanned. The resulting ring electrode current, when plotted vs. the disk electrode potential, gives a complete picture of the conditions which are required to form the species B.

Ring collection experiments are free of double layer charging effects, except under special circumstances.[10-12]

One of the earliest examples of such an experiment was performed by Nekrasov and Berezina;[13] in it Cu(I)

(9) W. J. Albery and S. Bruckenstein, *Trans. Faraday Soc.*, 62, 1920 (1966).
(10) M. S. Shabrang and S. Bruckenstein, *J. Electrochem. Soc.*, 121, 1439 (1974).
(11) M. S. Shabrang and S. Bruckenstein, *J. Electrochem. Soc.*, 122, 1305 (1975).
(12) W. J. Albery, A. H. Davis, and A. J. Mason, *Discuss. Faraday Soc.*, 56, 317 (1973).
(13) L. N. Nekrasov and N. P. Berezina, *Dokl. Akad. Nauk SSSR*, 142, 855 (1962).

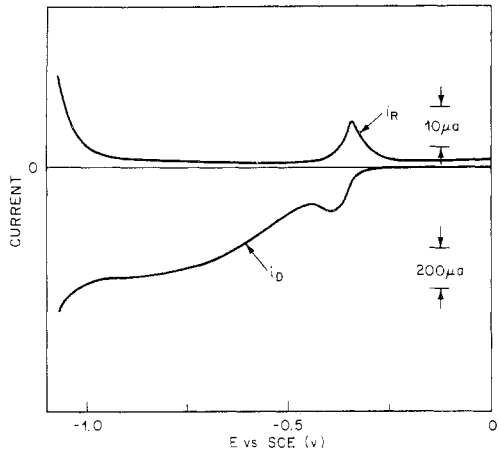

Figure 3. Disk current under potential-controlled scan at 2.5 mV/s and ring current at +0.3 V vs. SCE for 2 mM $CuSO_4$ in 0.1 M H_2SO_4. Rotation speed 3600 rpm; Pt disk–Pt ring; current sensitivities as indicated.

was detected as an intermediate escaping a disk electrode during the reduction of Cu(II) to copper metal in Na_2SO_4 solution. Figure 3 contains the i_D–E_D curve obtained in our laboratories for the reduction of Cu(II) in 0.1 M H_2SO_4. The corresponding i_R–E_D curve was obtained at a ring potential where the oxidation of Cu(I) to Cu(II) occurs. The disk potential range over which Cu(I) occurs as an intermediate in the reduction of Cu(II) to copper is clearly defined. The initial stages of this reduction process remain incompletely understood. At very cathodic disk potentials, the evolution of hydrogen is detected by its anodic oxidation at the ring.

The ability to detect small amounts of Cu(I) by oxidizing it at a ring electrode was employed advantageously to study the equilibrium constant for the reaction Cu + Cu(II) $\rightleftarrows$ 2Cu(I) using a copper disk–platinum ring electrode.[14]

Shielding Experiments. A "shielding" experiment normally involves setting $E_R = E_D$. Under these conditions the shielded ring electrode current, $(i_R)_{SH}$, is less than i_R (eq 3) because some A is removed from solution at the disk electrode by conversion to B, as depicted in Figure 1. The shielded current can be expressed in several equivalent ways.[15,16]

$$(i_R)_{SH} = i_R - Ni_D = (\beta^{2/3} - N)i_D \qquad (7)$$

Close Relation between Collection and Shielding. In Figure 2, the relationships existing at various potentials are shown for (I) the disk electrode i_D–E_D curve, (II) the ring electrode i_R–E_R curve in the absence of a disk, and (III) the ring electrode i_R–E_R curve for the case of an applied disk potential, E_1, on the limiting current $[(i_D)_L]$ region for the reduction of species A. Only A is assumed to be present in the bulk of solution. Curve III is shifted anodically in current by an amount equal to $N(i_D)_L$ as compared to curve II. At all potentials cathodic to E_1, the ring current is fully shielded, while the ring electrode collection current is developed at potentials more anodic than E_2. Such behavior is found for redox systems free of adsorption and kinetic complications.[16,17]

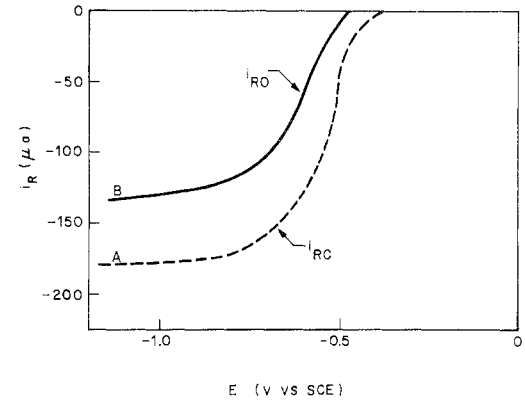

Figure 4. Ring potential scans at 10 mV/s for a Zn disk–Cu ring electrode rotated at 1600 rpm in air-saturated 0.5 M KCl. (A) Zn disk lacquer coated; (B) Zn disk exposed.

Shielding experiments make it possible to determine precisely how much of an electroactive species is consumed at the disk electrode. Species A reacts by a current consuming faradaic process in reaction 1. However, if A were to be removed by a non-current-consuming process at the disk electrode, e.g., by a chemical reaction or adsorption at the disk electrode, the value of i_R would still be decreased to $(i_R)_{SH}$.

Corrosion of Zinc. One unpublished shielding example involves the reaction of oxygen with a zinc disk electrode. This reaction is a typical corrosion process and proceeds according to eq 8. The presence of O_2

$$2Zn + O_2 + 4H^+ = 2Zn^{2+} + 2H_2O \qquad (8)$$

severely interferes with measuring the ring collection of Zn^{2+} by reduction. However, the oxygen consumed can be determined using a copper ring electrode in a shielding experiment. Thus, the difference in the ring currents for oxygen reduction, detected as in Figure 4, with no disk (i.e., lacquer covered) and a zinc disk, agree quantitatively with eq 7. This result clearly demonstrates that the corrosion mechanism is a convective-diffusion-limited reduction of oxygen.

The advantages of the RRDE shielding technique have been little exploited, and there are a variety of difficult-to-follow heterogeneous chemical processes whose equilibrium and kinetic parameters have now become readily accessible.

In the above discussion, we have assumed that the product of the disk electrode reaction is stable. Frequently this is not the case, and reactions in transit from disk to ring may alter the ring current.

The literature is replete with various theoretical and experimental examples of using the angular velocity dependence of the ring current to identify electrode intermediates and to investigate the details of electrochemical reactions.[18,19] This topic will not be further discussed here. However, there is little doubt that this particular phase of RRDE methodology is being accepted as a standard tool in electrochemical studies.

Relations of Currents and Fluxes. Another key problem in analyzing a complicated electrochemical reaction involves separating out the fluxes at an elec-

(14) G. W. Tindall and S. Bruckenstein, *Anal. Chem.*, **40**, 1402 (1968).
(15) S. Bruckenstein, *Electrokhimiya*, **9**, 1085 (1966).
(16) W. J. Albery and S. Bruckenstein, *Trans. Faraday Soc.*, **62**, 1932 (1966).
(17) D. T. Napp, D. C. Johnson, and S. Bruckenstein, *Anal. Chem.*, **39**, 481 (1967).
(18) W. J. Albery and M. L. Hitchman, "Ring-Disk Electrodes", Oxford University Press, London, 1971, pp 73–133.
(19) R. N. Adams, "Electrochemistry at Solid Electrodes", Marcel Dekker, New York, N.Y., 1969, pp 110–114.

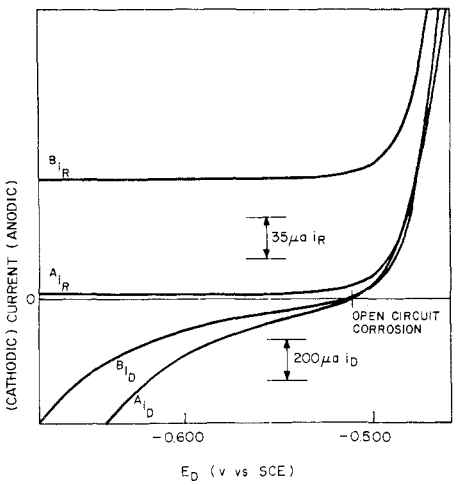

Figure 5. Disk potential scans (A_{i_D} and B_{i_D}) at 10 mV/s for Fe disk–Au ring electrode. Ring potential held at +1.0 V vs. SCE; ring current traces A_{i_R} and B_{i_R}. Solutions 1 M H_2SO_4 (A curves), 1 mM $FeSO_4$ + 1 M H_2SO_4 (B curves). Rotation speed 1600 rpm; current sensitivites as indicated.

trode that generate (or consume) current, as measured in the external circuit, from those that do not generate (or consume) current. The latter complication can arise from adsorption/desorption processes and homogeneous and surface reactions, one example of which is the corrosion of zinc by oxygen as discussed above.

The total measured external current at the disk of a RRDE is the sum of five components: (a) convective-diffusion currents described by the Levich equation; (b) surface process currents associated with the oxidation or reduction of the electrode itself; (c) adsorption currents associated with the oxidation or reduction of adsorbed species; (d) double layer charging currents which arise because of the electrochemical potential (or current) control program imposed on the disk; and (e) currents arising from the supporting electrolyte which may be kinetically controlled. The observed ring electrode current at a RRDE arises from the same sources as the total disk current, except that the convective-diffusion-controlled currents are modified by shielding and collection phenomena.

The flux of electroactive material reaching the ring electrode originates from two sources: (a) the flux originating from disk processes that produce soluble species which are then conveyed to the ring by convective diffusion, and (b) the flux from species originally present in the bulk solution.

The value of the disk component of the ring flux is determined by N and the chemical reactions a species undergoes in transit from disk to ring. Since this flux may arise either from a current-producing electron-transfer reaction or from a non-current-type reaction at the disk electrode, it is in general not possible to predict the experimental ring current component from N and a disk current. Rather, we compare the experimental disk current with the disk current obtained by dividing N into the ring current, and thus obtain quantitative information about non-current-type disk electrode processes.

Corrosion of Iron. An example of deducing the chemical reactions occurring at a disk from ring measurements is given by the dissolution of iron in 1.0 M H_2SO_4 and in 1.0 M H_2SO_4 + 1 mM Fe(II). The i–E curves obtained at an iron disk–gold ring RRDE are presented in Figure 5. The presence of Fe(II) has little effect on the disk curves. The differences in the disk scans are due mainly to the result of the surface changes.

Curves A_{i_R} and B_{i_R} are the i_R–E_D curves obtained simultaneously with i_D–E_D curves A_{i_D} and B_{i_D} at a ring electrode potential where Fe(II) is oxidized to Fe(III). The gold ring is unresponsive to hydrogen oxidation. Inspecting curves A_{i_R} and A_{i_D} we see that there is a ring collection current for Fe(II) near the disk electrode open circuit potential, even though there is no net anodic disk current. This ring collection current arises from the flux of Fe(II) generated at the disk electrode by the electrochemically controlled process (eq 9). At disk po-

$$Fe + 2H^+ = Fe(II) + H_2 \qquad (9)$$

tentials positive of the open circuit potential, Fe(II) is produced via anodic oxidation of the iron disk, as is confirmed by the additional ring collection current predicted by eq 6. In the presence of Fe(II), curve B_{i_R} is displaced from curve A_{i_R} by a constant amount because of the oxidation of additional Fe(II) arriving at the ring from the bulk of the solution.

Underpotential Deposition of Metals. Examples of the application of the concepts discussed above exist in the studies of the underpotential deposition of metals. It is now generally recognized that the initiation of the deposition of one metal, M, on another may begin many hundreds of millivolts more anodic than the reversible potential for the M^{n+}/M couple[20,21] and is easily detected by shielding experiments. After several atom layers of M are deposited, the equilibrium potential is reached and bulk M is deposited.

The explanation of this important phenomenon is still a matter of dispute.[22-24] However, such underpotential phenomena are important in a variety of electrochemical processes, including electrocatalysis.[25] The RRDE can be definitive in correlating kinetic effects with underpotential processes, and the poisoning of the oxygen reduction reaction on platinum is one such example.[26]

Poisoning of Oxygen Reduction. In 0.2 M H_2SO_4 oxygen is reduced at platinum to water (E = 0.0 V vs. SCE) in a convective-diffusion-controlled process. In the same supporting electrolyte plus 2×10^{-5} M Cu(II), in the presence and absence of oxygen, a monolayer of underpotential copper can be deposited (E = 0.0 V vs. SCE). A cathodic current for Cu(II) reduction flows only while the monolayer is forming, since bulk copper does not deposit unless the electrode potential is somewhat more cathodic than 0.0 V.

Figure 6 shows current transients obtained at a RRDE in air-saturated 0.2 M H_2SO_4 + 2.0×10^{-5} M Cu(II). The copper ring is held at −0.25 V, where the reaction Cu(II) + 2e = Cu occurs. Oxygen is not reduced under these conditions on copper. The potential

(20) M. Haissinsky, *J. Chim. Phys. Phys.-Chim. Biol.*, **43**, 21 (1946).
(21) L. B. Rogers, D. P. Krause, J. C. Griess, Jr., and D. B. Ehlinger, *J. Electrochem. Soc.*, **95**, 33 (1949).
(22) H. Gerischer, D. M. Kolb, and M. Przasnyski, *Surf. Sci.*, **43**, 662 (1974).
(23) A. K. Vijh, *Surf. Sci.*, **47**, 709 (1975).
(24) D. M. Kolb, M. Przasnyski, and H. Gerischer, *J. Electroanal. Chem.*, **54**, 25 (1974).
(25) R. R. Adzic and A. R. Despic, *J. Chem. Phys.*, **61**, 3482 (1974).
(26) G. W. Tindall, S. H. Cadle, and S. Bruckenstein, *J. Am. Chem. Soc.*, **91**, 2119 (1969).

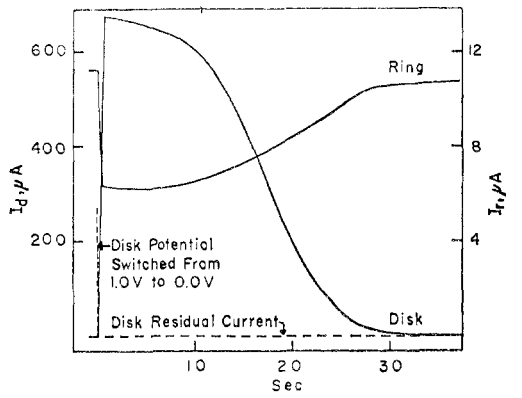

Figure 6. Time dependence of the oxygen reduction current at the disk and the Cu(II) reduction current at the ring of a platinum ring–disk electrode. Solution 0.2 M H_2SO_4 and 2×10^{-5} M Cu(II) with air saturation. Rotation speed 2500 rpm. Disk potential held at 0.00 V vs. SCE for $t > 0$; ring potential = −0.25 V vs. SCE at all t. Disk area 0.458 cm^2, $\beta^{2/3} = 0.36$, collection efficiency 0.183.

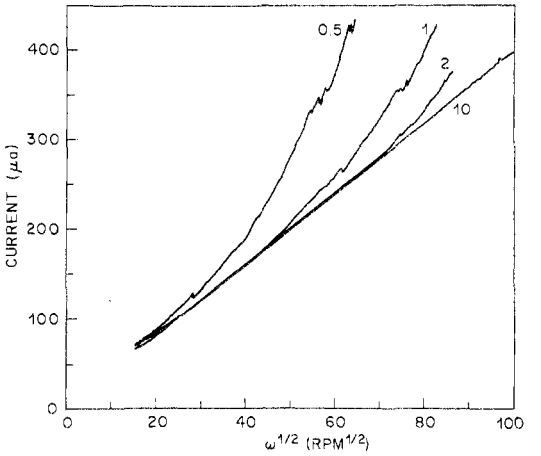

Figure 7. Deposition current vs. $\omega^{1/2}$ for silver reduction onto a 0.311 cm^2 platinum disk in 0.5 mM $AgNO_3$–1 M KNO_3 solution. Speed scan rate in rpm$^{1/2}$ sec^{-1} indicated on traces. Controlled potential −0.65 V vs. Ag wire reference.

of the platinum disk is initially at 1.0 V, where no reaction occurs and no copper is adsorbed. Its potential is then stepped to 0.0 V, and oxygen reduction begins, along with underpotential copper deposition. Since the oxygen concentration is much higher than that of Cu(II), the disk current is almost completely due to oxygen reduction. At the same time as the potential step, the ring current goes from an unshielded to a shielded state because Cu(II) is consumed at a limiting current level at the disk. As the underpotential deposition process proceeds on the disk toward equilibrium monolayer coverage, the ring current shields. After one monolayer coverage is attained, Cu(II) consumption at the disk ceases, and the ring current returns to the value for an isolated ring detecting 2×10^{-5} M Cu(II). The decrease in the disk electrode oxygen reduction current parallels the unshielding of the ring electrode current, unequivocally demonstrating the relationship between the poisoning of the oxygen reduction process and the underpotential deposition of copper.

Hydrodynamic Control of Flux

Rationale. Electrochemists are often interested in studying the electron-transfer reaction represented by eq 1 at solid electrodes in the presence of other complicating processes. The observed current is, in fact, the sum of several contributions, as discussed earlier.

The RDE is capable of distinguishing the convective-diffusion-controlled current from all others, but conventional experimental techniques introduce a variety of uncertainties that interfere with such a separation. Dynamic control of the rotation speed of a RDE minimizes these errors.[27-32]

In eq 1 assume that the reaction proceeds at an appreciable rate and that A and/or B are soluble species. The flux of electroactive material and associated current will depend upon the rotation speed, linearly with $\omega^{1/2}$ for a reversible process. The other processes giving rise to currents are either totally independent of ω (double layer charging and adsorptive processes) or nearly independent of ω if, as is frequently found (supporting electrolyte and surface reactions), they arise from kinetically controlled processes. Thus, in principle, i_D–E_D curves might be obtained at two rotation speeds and their difference taken to get a Δi–E curve showing only the ω-dependent current associated with eq 1. Unfortunately, this approach is severely limited because the convective and non-convective-diffusion-controlled currents often change at solid electrodes within the time of two successive experiments. For example, if unsuspected impurities adsorb and poison the electrode process, the current response of the solid electrode can change rapidly, as has been observed during the reduction of oxygen on platinum[33] and of Fe(III) on gold.[34] Also, geometric changes alter the hydrodynamic conditions. Thus, the formation of metal dendrites, as occurs when silver deposits on platinum from potassium nitrate solution, produces a time-dependent current.

Automated Levich Plots. Programming the rotation speed as a function of time permits recording i_D vs. $\omega^{1/2}$ plots very rapidly, which avoids the problem of passing enough coulombs to alter the physical state of the surfaces. Various control approaches have been used, with ω being linearly scanned vs. t, t^2, and $\exp(kt)$.[27,28]

Figure 7 shows the results of acquiring i_D vs. $\omega^{1/2}$ data for the reduction of Ag^+ in KNO_3 on platinum with a $\omega \propto t^2$ program. Linear Levich plots yielding the accepted diffusion coefficient of Ag^+ are obtained only for fast scanning speeds ($t < 10$ s in going from 400 to 10 000 rpm). At lower scanning speeds the growth of silver dendrites leads to excessive currents with time, as is also the case with manual measurements.

Control of Surface Concentration. The determination of the surface concentrations of kinetically active species is essential in electrochemical studies. ω

(27) S. C. Creason and R. F. Nelson, *J. Electroanal. Chem.*, **21**, 549 (1969).
(28) B. Miller, M. I. Bellavance, and S. Bruckenstein, *Anal. Chem.*, **44**, 1983 (1972).
(29) B. Miller and S. Bruckenstein, *J. Electrochem. Soc.*, **117**, 1032 (1970).
(30) B. Miller and S. Bruckenstein, *Anal. Chem.*, **46**, 2026 (1974).
(31) B. Miller and S. Bruckenstein, *J. Electrochem. Soc.*, **121**, 1558 (1974).
(32) K. Tokuda, S. Bruckenstein, and B. Miller, *J. Electrochem. Soc.*, **122**, 1316 (1975).
(33) D. C. Johnson and S. Bruckenstein, *Anal. Chem.*, **43**, 1313 (1971).
(34) B. Miller, M. I. Bellavance, and S. Bruckenstein, *J. Electrochem. Soc.*, **118**, 1082 (1971).

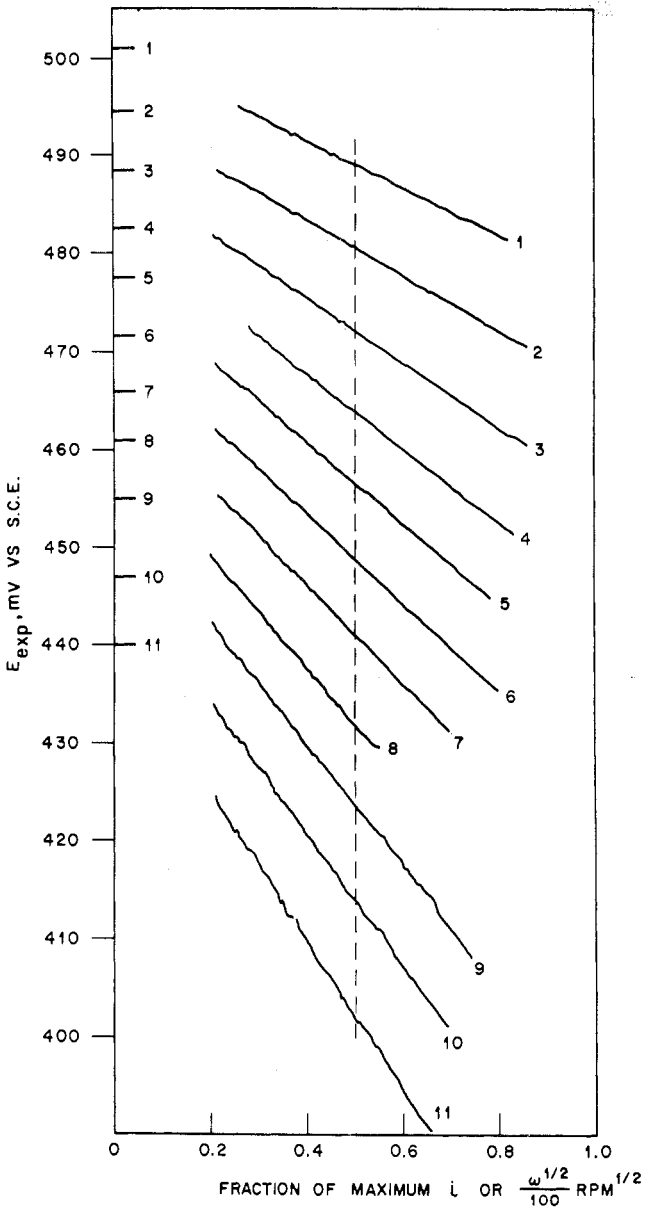

Figure 8. ISCVA data for 9.7 mM Fe(III) in 0.1 M HCl–1.0 M NaCl solution at gold at different values of limiting current fraction, f. Actual data shown. E_{eq} obtained by the extrapolation to zero current of each tracing is indicated. f values for the experimental lines are (1) 0.260, (2) 0.312, (3) 0.364, (4) 0.416, (5) 0.468, (6) 0.520, (7) 0.572, (8) 0.624, (9) 0.676, (10) 0.728, (11) 0.780. Vertical dashed line intercepts are E_{exp} values at 2500 rpm. Plots of E vs. log $(1-f)/f$ yielded a slope of 0.060 V/decade at 25 °C where E was the intercept value and a slope of 0.086 V/decade where E was the 2500 rpm value, confirming the predictions of theory.

programming can simplify the mathematical problem by using a control function suggested by rotating disk theory and also reduce the sensitivity of the kinetic experiments to impurity and other time-dependent effects. As can be seen from eq 2 the surface concentration of an electroactive species may be held constant at a predetermined value by fixing the ratio of $i_D/\omega^{1/2}$ while i_D (and thus $\omega^{1/2}$) is scanned linearly with time (isosurface concentration voltammetry, ISCVA). The resultant plots of E_D vs. i_D for different $i_D/\omega^{1/2}$ ratios yield the relevant kinetic and thermodynamic information. Such data are shown in Figure 8 for the Fe(III)/Fe(II) system at a gold electrode in

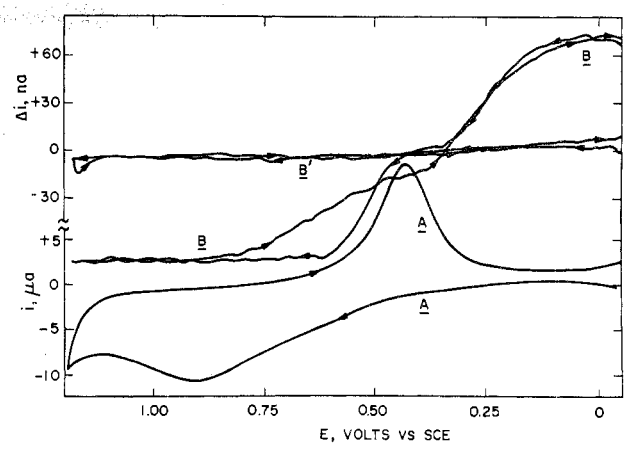

Figure 9. RDE and SHM curves for quinhydrone at platinum. Curve A, conventional cyclic potential scan of 1.00 μM quinhydrone at platinum RDE in 0.02 M H_2SO_4. Curve B, SHM trace for curve A solution. Curve B′, SHM residual in 0.02 M H_2SO_4. Conditions: $\omega_0^{1/2}$ = 60 rpm$^{1/2}$, $\Delta\omega^{1/2}$ = 6 rpm$^{1/2}$, modulation frequency = 3 Hz, scan rate = 5 mV/s, averaging time constant for modulated current = 3 s.

acid chloride medium. The slopes, which have the dimensions of resistance, are a measure of the resistance to electron transfer across the electrode solution interface, and the rate constant for electron transfer is calculated from these slopes.[34]

The zero current intercepts, labeled 1 to 11 on the potential axis, are the equilibrium potentials for the particular surface concentrations of Fe(III) and Fe(II) set by the $i_D/\omega^{1/2}$ ratio and yield $E°$.

The ISCVA technique could also be applied advantageously (1) to study the kinetics and thermodynamics of a couple whose components undergo reaction after leaving the diffusion layer and (2) to make measurements in resistive supporting electrolytes where other techniques are less satisfactory.

Sinusoidal Modulation of Rotation Speed. A powerful extension of rotation speed programming is the sinusoidal variation of $\omega^{1/2}$ about a fixed center speed ($\omega_0^{1/2}$) with peak-to-peak amplitude, $\Delta\omega^{1/2}$, to give

$$\omega^{1/2} = \omega_0{}^{1/2}(1 + \epsilon \sin \sigma t) \qquad (10)$$

where

$$\epsilon = \Delta\omega^{1/2}/\omega_0{}^{1/2} < 1 \text{ (typically } \epsilon \sim 0.05) \qquad (11)$$

and σ is the radian frequency of $\omega^{1/2}$ modulation.

The time-dependent current response ($i(t)$), assuming the Levich equation applies, is given by eq 12 and the

$$i(t) = i_{\omega_0}(1 + \epsilon \sin \sigma t) \qquad (12)$$

peak-to-peak response (Δi) is given by eq 13. This

$$\Delta i = \epsilon i_{\omega_0} = \frac{\Delta\omega^{1/2}}{\omega^{1/2}} i_{\omega_0} \qquad (13)$$

experiment has been termed sinusoidal hydrodynamic modulation (SHM). SHM has been implemented and found to yield excellent Δi–E data at the submicromolar concentration level, even in the presence of extreme surface complications and large kinetically controlled currents.[28,30]

Figure 9 shows SHM results obtained in the study of quinhydrone at a platinum electrode. Curve A is the conventional i_D–E_D curve for micromolar quinhydrone in 0.01 M $HClO_4$. There is no detectable difference

Table I
Rotating Electrode Applications

Classical		Hydrodynamic control	
RDE	RRDE	SHM (periodic)	Scanned programs
Electroanalysis[c]	Flux consumed or produced at disk[4,14,a]	Isolation of convective diffusion current[30,34]	Automated Levich plots[27-29]
D[6,8] or n[8]	Reaction intermediate identification[13,h]	No double-layer charging[28,30]	Automated i^{-1} *vs* ω^{-1} plots for kinetics[u]
Kinetics[18,19]	Kinetics, mechanisms and rates[a,b]	Rejection of surface and irreversible supporting electrolyte currents, extension of practical limits[30]	Hydrodynamic potentiometry[29]
Corrosion[d-f]	Film solubility[i]	Trace and microanalysis[30]	Isosurface concentration voltammetry (kinetics, equilibrium potentials)[34]
Solubility[g]	Adsorption[a]	Reaction on changing electrode surfaces[30]	
	Underpotential deposition[j]	Kinetic methods[31]	
	Diffusion layer titrations[a]	D from relaxation as a function of frequency[32]	
	Transit phenomena[k]		
	Potentiometry[l]		
	Heterogeneous equilibria[14]		
	Corrosion rates[m]		
	Split-ring; alloy- or time-dependent phenomena independent of n[n]		
	Passivation mechanism, stripping studies[o]		
	Alloy selectivity in dissolution[p,q]		
	Simulations[r]		
	Current distribution studies from shielding[s,t]		

[a] See Albery and Hitchman.[18] [b] See Adams.[19] [c] L. Meites, "Polarographic Techniques", Interscience, New York N.Y., 1965, Chapter 8. [d] Z. Zembura, *Corros. Sci.*, **8**, 703 (1968). [e] Z. Zembura, *Electrochim. Acta*, 10, 859 (1965). [f] A. C. Riddiford, *Adv. Electrochem. Electrochem. Eng.*, 4, 47 (1966). [g] H. G. Linge and G. H. Nancollas, *Calcif. Tissue Res.*, 12, 193 (1973). [h] L. N. Nekrasov and L. Muller, *Dokl. Akad. Nauk SSSR*, 142, 855 (1962). [i] B. Miller, *J. Electrochem. Soc.*, 117, 491 (1970). [j] V. Vicente and S. Bruckenstein, *Anal. Chem.*, **45**, 2036 (1973). [k] G. A. Feldman and S. Bruckenstein, *J. Electroanal. Chem.*, 9, 395 (1965). [l] W. J. Albery and S. Bruckenstein, *Trans. Faraday Soc.*, 62, 1932 (1965). [m] B. Miller, *J. Electrochem. Soc.*, **119**, 1510 (1972). [n] B. Miller, *J. Electrochem. Soc.*, 116, 1677 (1969). [o] Y. Okinaka, *J. Electrochem. Soc.*, 117, 289 (1970). [p] H. W. Pickering, *J. Electrochem. Soc.*, 114, 698 (1967). [q] H. G. Feller, *Z. Metallkd.*, **58**, 5875 (1967). [r] K. B. Prater and A. J. Bard, *J. Electrochem. Soc.*, **117**, 1517 (1970). [s] W. J. Smyrl and J. Newman, *J. Electrochem. Soc.*, **119**, 208 (1974). [t] W. J. Smyrl and J. Newman, *J. Electrochem. Soc.*, 119, 211 (1974). [u] K. J. Kretchmer, C. H. Hamman, and B. Fassbender, *J. Electroanal. Chem.*, **60**, 231 (1975).

between this curve and that without quinhydrone as the current is almost entirely due to platinum surface oxidation and reduction. Curves B and B′ are the corresponding SHM curves, and the well-developed Δi–E curve recovered for quinhydrone agrees with eq 2. The usable analytical sensitivity of solid electrodes has been increased 100-fold by using the SHM procedure. Other examples bearing out the selectivity of the SHM procedure for convective diffusion processes have been obtained at various electrode materials[30] and make possible otherwise impractical voltammetric studies.

SHM is also useful for the study of electron-transfer kinetics.[31] This theory has been given and verified for the situations where both A and B are soluble species and where one of them is a solid.[31] The SHM experiment tends to emphasize kinetic behavior when compared to a conventional i_D–E_D curve and measures somewhat faster rate constants. Thus, SHM kinetic studies are especially useful when nonconvective and convective processes occur simultaneously with the electron-transfer process.

Levich's derivation of eq 2 assumed a convective-diffusion "steady state". However, for any particular value of ω_0, there is a value of σ for which this assumption fails. These σ effects have been examined and interpreted recently.[32] There are experimental advantages to using high values of the ratio σ/ω, despite increased mathematical complications. First, the signal processing technique is somewhat simpler with increasing modulation frequency. Second, the shortened experimental time scale makes it possible to study electrochemical processes in the presence of other complicating and poisoning processes. Third, the diffusion coefficient can be calculated without a priori knowledge of the number of electrons involved in the overall electrode process. Fourth, σ effects are likely to prove diagnostic of the electrochemical reaction mechanism.

Complementarity of Classical and Hydrodynamically Programmed Rotating Electrodes

Rotating electrode methodologies have evolved to the promising status outlined above. Further details are given in Table I which lists selected classical voltammetric uses of the RDE and RRDE along with some of the newer applications made possible by programmed control of the system hydrodynamics. Our tabulation is not intended to be comprehensive or indicate historical priority. Rather it is meant to suggest the scope of the present uses of rotating electrodes and thus other likely applications. Fruitful extensions of the rotating disk system, such as the use of ac potential or current signals, impedance techniques, and optically transparent disks or rings are only a few of the promising approaches we have not considered here.

Classical RDE experiments measure those terms in which the current is explicitly defined in the Levich equation, such as n_D, D, and bulk concentration. They have been used to determine the net overall electrochemical reaction and the transport properties of the electrochemical species, and for solution analysis. Classical RDE kinetic studies at constant potential have

exploited the use of different constant rotation speeds by extrapolating current data to infinite rotation speed ($1/\omega \rightarrow 0$), thus eliminating the difference between surface and bulk concentrations.

These rotating solid electrode techniques are still subject to interferences from nonfaradaic and time-varying surface-process currents. Therefore, despite their inherent advantages of high sensitivity and different potential range, they have always suffered when compared to the atomically smooth, constantly renewing dropping mercury electrodes. Hydrodynamic programming, particularly in the SHM mode at the RDE, has made great strides in eliminating many solid electrode disadvantages. The unique prospects of controlled surface concentrations via ω–f(i) programming have added to the controlled potential and current techniques for electrochemical studies. Also $\omega^{-1/2}$ control now provides a variable comparable to time.[29]

It is apparent from the list of RRDE applications that the virtually instantaneous analysis of the diffusion layer provided by the ring adds immensely to the range of chemical and mechanistic problems that can be studied. Also the complementary relationship of the RRDE and hydrodynamic voltammetric methodologies suggests that even more subtle problems can be attacked by applying the methods in concert.

Stanley Bruckenstein is grateful to Bell Laboratories for their hospitality during the period in which the work on this paper was done.

Selective Dissociation of Polyatomic Molecules by Intense Infrared Laser Fields

Rafael V. Ambartzumian and Vladilen S. Letokhov*

Institute of Spectroscopy, Academy of Sciences USSR, Moscow, USSR

Received July 22, 1976

In this Account we discuss the specific features of the isotopically selective dissociation of polyatomic molecules (BCl_3,[1] SF_6,[2] OsO_4,[3] etc.) by intense CO_2 laser pulses. The effect was discovered in 1974 in our laboratory. Though for some people our discovery was perhaps unexpected, for us it was, in fact, a logical and related result of our work on the isotopically selective dissociation of molecules by laser radiation. Accordingly, a short review of the development of our work is appropriate here.

In 1970 we began systematic studies of isotopically selective molecular dissociation based on selective excitation of molecular vibrational levels and subsequent dissociation of selectively excited molecules by UV radiation (two-step IR–UV dissociation). The first results of this work were reported in 1971 at the CLEA conference,[4] and after a year our laboratory realized what was perhaps the first successful isotope separation (^{14}N and ^{15}N) by the method of two-step selective dissociation of molecules (NH_3).[5] At approximately the same time we realized that in some cases isotopically selective dissociation was possible in a one-step process owing to the effect of predissociation.[6] The first successful experiment on isotope separation by this technique was also carried out in 1972, by Yeung and Moore.[7] Thus, in addition to the well-known photochemical approach to isotope separation, a new photodissociation method was developed (see reviews[8,9]). This method has basic advantages over the photochemical one as far as high selectivity is concerned, because it employs chemical binding of dissociation products and does not necessitate special selection of a fast reaction of selectively excited atoms or molecules.[10]

In 1971 we began studying the visible luminescence of molecular gases pumped by focused CO_2 laser pulses. This phenomen had been observed by Isenor and Richardson[11] not long before. We made a detailed study of the kinetics and spectra of luminescence of NH_3 and C_2F_3Cl molecules pumped by transversely excited atmospheric pressure (TEA) CO_2 laser pulses[12,13] (similar experiments are described in ref 14). In this

V. S. Letokhov is Vice Director and Head of the Laser Spectroscopy Laboratory of the Institute of Spectroscopy, Academy of Sciences USSR. He was born near Irkutsk, Siberia, and graduated from Moscow Physical Technical Institute. He received his Ph.D. degree in 1969 from Lebedev Physical Institute with N. G. Basov. Dr. Letokhov's research interests are in laser frequency standards, high power lasers, and selective laser photochemistry and photophysics.

R. V. Ambartzumian was born in Leningrad and graduated from Moscow University. After receiving the Ph.D. degree from Lebedev Physical Institute in 1970, also with Professor Basov, Dr. Ambartzumian joined the Institute of Spectroscopy as Head of the Spectroscopy Excited States Laboratory. His research interests are in nonlinear amplification of laser pulses, laser frequency standards, and isotope selective photochemistry.

(1) R. V. Ambartzumian, V. S. Letokhov, E. A. Ryabov, and N. V. Chekalin, *Pis'ma Zh. Eksp. Teor. Fis.*, **20**, 597 (1974).
(2) R. V. Ambartzumian, Yu. A. Gorokhov, V. S. Letokhov, and G. N. Makarov, *Pis'ma Zh. Eksp. Teor. Fiz.*, **21**, 375 (1975).
(3) R. V. Ambartzumian, Yu. A. Gorokhov, V. S. Letokhov, and G. N. Makarov, *Pis'ma Zh. Eksp. Teor. Fiz.*, **22**, 96 (1975).
(4) R. V. Ambartzumian and V. S. Letokhov, *IEEE J. Quant. Electron.*, **QE-7**, 305 (1971); *Appl. Opt.*, 11, 354 (1972).
(5) R. V. Ambartzumian, V. S. Letokhov, G. N. Makarov, and A. A. Puretzkii, *Pis'ma Zh. Eksp. Teor. Fiz.*, **15**, 709 (1972); **17**, 91 (1973).
(6) V. S. Letokhov, *Chem. Phys. Lett.*, **15**, 221 (1972).
(7) E. S. Yeung and C. B. Moore, *Appl. Phys. Lett.*, **21**, 109 (1972).
(8) V. S. Letokhov, *Science*, **180**, 451 (1973); C. B. Moore, *Acc. Chem. Res.*, **6**, 323 (1973).
(9) V. S. Letokhov and C. B. Moore, *Kvantovaya Elektron. (Moscow)*, **2**, 248 (1976); **2**, 485 (1976); Preprint LBL-4904 (English), March 1976.
(10) V. S. Letokhov, "Principles of Laser Isotope Separation" (Lectures in Les-Houches Summer School of Theoretical Physics, July 1975, Les-Houches, France), North-Holland Publishing Co., Amsterdam, 1976, in press.
(11) N. R. Isenor and M. C. Richardson, *Appl. Phys. Lett.*, **18**, 224 (1971).
(12) V. S. Letokhov, E. A. Ryabov, and C. A. Tumanov, *Opt. Commun.*, **5**, 168 (1972).
(13) V. S. Letokhov, E. A. Ryabov, and O. A. Tumanov, *Zh. Eksp. Teor. Fiz.*, **63**, 2025 (1972).